Geophysical Research Letters

RESEARCH LETTER
10.1029/2019GL082463

The Polar Stratosphere as an Arbiter of the Projected Tropical Versus Polar Tug of War

Yannick Peings[1], Julien Cattiaux[2], and Gudrun Magnusdottir[1]

[1]Department of Earth System Science, University of California, Irvine, CA, USA, [2]Centre National de Recherches Météorologiques, Université de Toulouse, CNRS, Météo-France, Toulouse, France

Key Points:
- The late 21st century temperature anomalies in the upper-level tropics and the Arctic are imposed in a high-top atmospheric model using nudging
- In winter, warmer tropics induce a weakening of the polar vortex that reinforces the response to Arctic amplification (no tug of war)
- The polar stratosphere has the potential to shape the tug of war over the North Atlantic in future climate scenarios

Supporting Information:
- Supporting Information S1

Correspondence to:
Y. Peings,
ypeings@uci.edu

Citation:
Peings, Y., Cattiaux, J., & Magnusdottir, G. (2019). The polar stratosphere as an arbiter of the projected tropical versus polar tug of war. *Geophysical Research Letters*, *46*, 9261–9270. https://doi.org/10.1029/2019GL082463

Received 14 FEB 2019
Accepted 26 JUL 2019
Accepted article online 1 AUG 2019
Published online 12 AUG 2019

Abstract This study explores the "tug of war" between the effects of Arctic amplification ("AA") and upper-troposphere tropical warming ("UTW") on the response of the future North Atlantic atmospheric circulation. The late 21st century AA and UTW temperature anomalies are imposed in a high-top atmospheric model by nudging the temperature. Two sets of experiments are performed, with and without feedback of the polar stratosphere to highlight its role in the response to UTW, AA, and both combined. With interactive polar stratosphere, UTW forces an equatorward shift of the eddy-driven jet that reinforces the response to AA. However, when the polar stratosphere feedback is suppressed, the response to UTW is opposite and reflects the previously identified tug of war between the effects of UTW and AA in midlatitudes. This study highlights that the polar stratosphere is a key component for future changes in the North Atlantic atmospheric circulation and that it must be accurately represented in climate change scenarios.

Plain Language Summary The jet streams are bands of strong westerly winds that drive weather patterns in midlatitudes. With climate change, they are expected to migrate poleward in association with an expansion of the tropical belt and amplified upper-level tropical warming (UTW). However, recent studies have pointed out that the fast warming in the Arctic (or Arctic Amplification, AA) may counteract this effect in winter. In this study we explore the respective and combined influence of UTW and AA by prescribing temperature anomalies in an atmospheric model that resolves the stratosphere. The focus is on the North Atlantic sector, where previous work had found a pronounced tug of war effect. In fall, in the absence of any significant response in the polar stratosphere, we retrieve well-established results, that is, a poleward shift of the midlatitude jet in response to UTW and an equatorward shift in response to AA. However, in winter UTW induces a robust weakening of the stratospheric polar vortex that shifts the jet equatorward and reinforces the effect of AA. Our study highlights that the polar stratosphere may significantly modulate the tropics-Arctic tug of war in the future, advocating for an accurate representation of stratospheric processes in climate models.

1. Introduction

A "tug of war" has been identified in climate projections, concerning the changes in the midlatitude atmospheric circulation. In the midlatitudes, the general response to increased greenhouse gases (GHGs) concentrations consists of an expansion of Hadley cells (Lu et al., 2007) and a poleward shift of the eddy-driven jet streams and storm tracks (e.g., Barnes & Polvani, 2013; Shaw et al., 2016). This response is associated with a pronounced warming at upper levels in the tropics (referred to as UTW, for upper-troposphere tropical warming, henceforth; Santer et al., 2017). However, Arctic amplification (AA, i.e., stronger warming in high latitudes due to various feedbacks; Serreze et al., 2009, Stuecker et al., 2018) has been suggested to oppose this response in the Northern Hemisphere. Indeed, General Circulation Model (GCM) experiments that isolate the impact of Arctic sea ice loss simulate weaker westerlies in midlatitudes and an equatorward shift of the jet streams in fall/winter, that is, a negative phase of the Northern Annular Mode or the North Atlantic Oscillation (NAO; Deser et al., 2015, Blackport & Kushner, 2017, Screen et al., 2018, Zappa et al., 2018). This competition between the effects of UTW and AA on the midlatitude circulation is one factor driving large uncertainties concerning changes in the jet stream/storm track characteristics in future scenarios (Barnes & Polvani, 2015; Harvey et al., 2013; Peings et al., 2017; Zappa & Shepherd, 2017).

Despite great progress on the topic in recent years, isolating the effect of AA from the effect of tropical expansion and UTW is challenging. Sea ice loss sensitivity experiments give excellent insights on the impact of AA

(Screen et al., 2018), but sea ice loss is only one aspect of AA; for example, high-latitude snow melt and water vapor transport also play a role. Moreover, in fully coupled GCMs, the response to Arctic sea ice loss is communicated to lower latitudes, where it induces warmer sea surface temperature (SST; Tomas et al., 2016). This indirect SST response has to be considered to isolate the effect of a warmer Arctic alone, since it is opposed to the direct effect of decreased sea ice in the Arctic (Blackport & Kushner, 2017). Using climate projections from the latest Coupled Model Intercomparison Project (CMIP5, Taylor et al., 2012), the role of UTW versus AA can also be isolated using a composite or "storyline" approach (Peings et al., 2018; Zappa & Shepherd, 2017). However, limited sample size in terms of models/ensemble members, especially after compositing based on large-scale drivers, may limit robustness in the results.

To add complexity to the issue, the circulation changes are asymmetric in longitude, such that the zonal mean response masks regional specifics and longitudinal sectors must be examined individually (Cattiaux et al., 2016; Peings et al., 2017). For example, in the Community Earth System Model Large Ensemble (CESM-LENS, Kay et al., 2015), at the end of the 21st century the North American sector exhibits a weaker and wavier westerly flow (Vavrus et al., 2017). However, the response over the North Atlantic sector is very different, with a narrowing and strengthening of the westerlies that is associated with reduced waviness and reduced occurrence of blockings (Peings et al., 2018). This is also a sector where coupling with the stratosphere has been shown to have a significant impact on the tropospheric response (Hitchcock & Simpson, 2014; Manzini et al., 2014; Peings et al., 2017; Zappa & Shepherd, 2017). Through its downward influence on the troposphere, the polar stratosphere is a source of uncertainty for climate change in midlatitudes since it does not exhibit a consistent response in climate change scenarios (Manzini et al., 2014; Simpson et al., 2018).

In the present study, we experiment with a novel approach to reveal the response of the large-scale atmospheric circulation to UTW and AA and assess the role of the polar stratosphere in the tug of war. We directly impose UTW and AA in a high- top atmospheric GCM by nudging the temperature in the regions of interest, with or without variability in the polar stratosphere. A related previously applied approach is to impose heating anomalies into simplified atmospheric GCMs (e.g., Butler et al., 2010; Wang et al., 2012). In particular, Butler et al. (2010) investigated the individual and combined influences of UTW, AA, and the polar stratosphere, on the zonal mean circulation using a dry dynamical core GCM. However, to our knowledge, this has never been done in a full atmospheric GCM that includes moist processes. Our focus in this study is on the North Atlantic sector, where competing effects of UTW, AA, and of the polar stratosphere have been found in climate change projections (Peings et al., 2018; Zappa & Shepherd, 2017).

2. Methods

2.1. Numerical Experiments

The numerical experiments are performed with the Specified-Chemistry Whole Atmosphere Community Climate Model (SC-WACCM). Compared to the standard WACCM, SC-WACCM has prescribed chemistry (rather than interactive), which allows for significantly lower computational costs while retaining almost identical stratosphere climatology and variability (Smith et al., 2014). The model includes 66 vertical levels with a top at 5.1×10^{-6} hPa (~140 km), with parametrizations of nonorographic gravity waves and turbulent mountain stress that allow for a realistic frequency in Sudden Stratospheric Warmings (Richter et al., 2010). The horizontal resolution is $1.9° \times 2.5°$ in latitude/longitude. A Quasi-Biennial Oscillation (QBO) is included by relaxing equatorial zonal winds between 86 and 4 hPa toward the climatological QBO cycle (~28 months) observed in radiosonde data.

Two sets of experiments have been carried out for this study:

1. The first set of experiments is run with a freely evolving stratosphere. The control run (CTL) consists of a 51-year simulation forced with year 2000 external forcings (GHGs, aerosols, and solar) and climatological sea surface temperature and sea ice concentration from the HadISST dataset (1979–2008 average annual cycle; Rayner et al., 2003). Three perturbation experiments are branched off from the control on 1 October. They each include 50 members starting from the 50 different 1 October initial conditions from CTL. The simulations are run until the end of March. In these three experiments, a regional nudging of the temperature is applied in the Arctic lower troposphere and/or the upper troposphere in the tropics in order to impose AA and UTW signals in the model and examine the response in the Northern

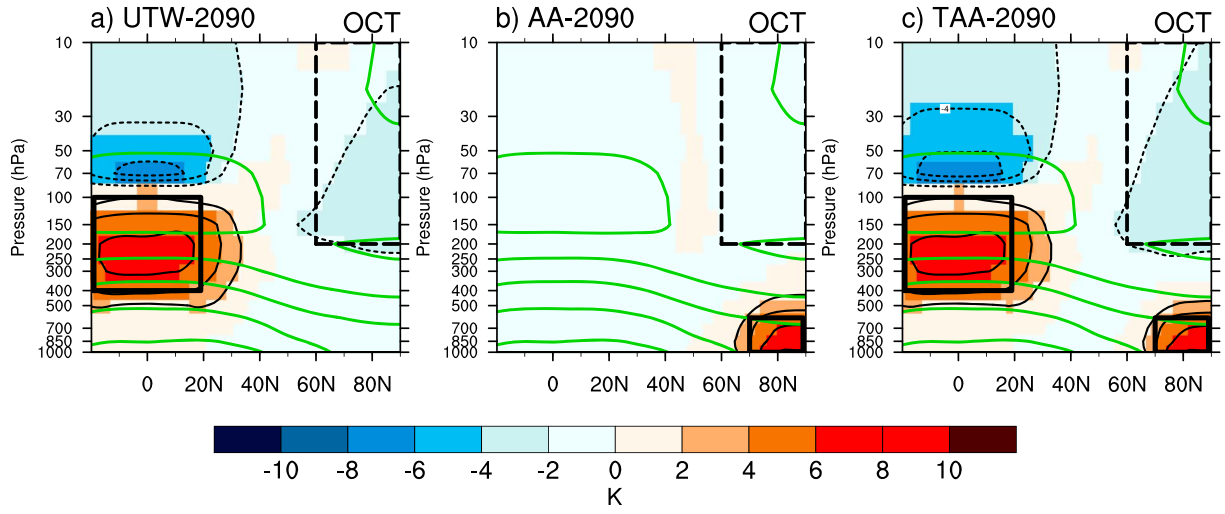

Figure 1. (a) October anomalies of the zonal mean temperature (K) in UTW-2090, with climatology from CTL shown in green contours (20 K interval from 210 K). The black box shows the nudging domain (dashed box is for the -cps experiments only). (b) Same as (a) but for AA-2090. (c) Same as (a) but for TAA-2090. UTW = upper-troposphere tropical warming; AA = Arctic amplification.

Hemisphere midlatitudes. The forcing consists of a smooth daily annual cycle of temperature anomalies that represent the projected change at the end of the 21st century (2080–2099 minus 1979–2008 averages) as projected by CESM-LENS (40-member ensemble mean). The daily anomalies from October to March are interpolated to 3-hr anomalies and superimposed on the 3-hr interpolated daily variability from the control run. This protocol allows us to retain high-frequency variability in the forced region, while imposing a background temperature anomaly. The temperature is relaxed at every model time step (30 min) with a relaxation coefficient of 0.1 (5 hr, i.e., 10 time steps, relaxation time). A buffer zone is applied at the limits of the nudging region to allow for a smooth linear transition from freely evolving to constrained grid points (see a full description of the nudging protocol in SI). The zonal mean temperature forcing and nudging domain for the three perturbation experiments are shown in Figure 1. The UTW forcing ("UTW-2090 experiment") is applied between 20°S and 20°N, from 400 to 100 hPa, and has a maximum of ~6 °C at 250 hPa at the equator (Figure 1a). The AA forcing ("AA-2090 experiment") is imposed north of 70°N, from the surface to 600 hPa and has the same maximum amplitude as UTW (Figure 1b). The "TAA-2090" experiment include both forcings (Figure 1c). These three experiments reveal the individual and combined impacts of UTW and AA on the large-scale atmospheric circulation in fall/winter. In order to verify the validity of the nudging protocol, we have run a nudging control simulation in which the temperature is nudged toward the control run daily variability (without superimposed temperature anomaly) in the UTW domain. When compared with the original control run, we did not find any significant tropospheric or stratospheric response (not shown), giving confidence that the nudging protocol does not create unwanted effects that may influence the results.

2. The second set of simulations includes similar temperature forcings as in UTW/AA/TAA-2090 but with imposed polar stratosphere to remove its influence on the tropospheric response. These three experiments are named UTW-2090-cps, AA-2090-cps, and TAA-2090-cps, with the "cps" suffix for "control polar stratosphere." In these experiments, the polar stratosphere (north of 65°N and above 200 hPa; see dashed box in Figure 1) is relaxed to the 3-hourly interpolated daily variability from CTL. They thus share similar polar stratosphere to CTL, and the polar stratosphere cannot respond to the imposed forcing. In these experiments the horizontal winds are also nudged in order to efficiently suppress any stratospheric variability. They reveal the role of the polar stratosphere in the atmospheric response to UTW and AA and in the tug of war between UTW and AA. For the sake of consistency, the -cps experiments are compared to a control run with similar relaxation of the polar stratosphere toward CTL but without any UTW or AA forcing applied. However, using the original control run as a reference does not affect the results since nudging the polar stratosphere toward CTL does not induce any significant response in the model.

2.2. Diagnostic Tools

For each experiment, a daily NAO index is defined as follows: We compute the first Empirical Orthogonal Function (EOF) mode of December–March sea-level pressure (SLP) in the (85°W/60°E; 20°N/85°N) domain in CTL. Daily NAO values are then obtained by projecting daily SLP anomalies on this EOF pattern. The wave activity in the extratropics is evaluated using the vertical component of the Plumb flux (Plumb, 1985) that characterizes the vertical propagation of wave-activity flux into the stratosphere.

3. Results

3.1. Individual and Combined Response to UTW and AA

A fast adjustment occurs in the stratosphere after applying UTW, with a cooling of the tropical stratosphere above the forcing and a cooling of the polar stratosphere, in October (Figure 1a). In AA-2090, the AA signal extends outside of the forcing region, with warm anomalies greater than 2°C north of 65°N and up to 400 hPa (Figure 1b). The response in TAA-2090 is a linear combination of the two forcings (Figure 1c), suggesting linear additivity in the effect of UTW and AA.

Figures 2a–2c show the response of the 700-hPa zonal wind (U700) in November over the North Atlantic sector in each experiment. UTW leads to reinforced westerlies on the poleward side of the eddy-driven jet, especially at the exit of the jet over the Norwegian and Barents Seas (Figure 2a). These anomalies represent a reinforcement and poleward extension of the eddy-driven jet, in line with the expected response to increased GHGs and warmer tropics in GCMs (McCusker et al., 2017; Oudar et al., 2017). In contrast, AA induces weaker westerlies on the poleward flank of the jet (Figure 2b). Decreased westerlies are found not only over the North Atlantic but also across all longitudes, consistent with increased tropospheric heights over the whole Arctic in AA-2090 (see Z500 anomalies in Figure S1 in the supporting information). In TAA-2090, the respective effects of UTW and AA cancel each other out, especially in the eastern and subpolar North Atlantic where no significant U700 anomalies are found (Figure 2c).

In winter (December to March average, DJFM), a completely new picture emerges in UTW-2090. A strong Rossby wave-like signal is found over the North Atlantic basin that projects onto the negative NAO (see also Z500 anomalies in Figure S1d) and results in a robust equatorward shift of the jet (Figure 2d). This response is robust over DJFM and also in each winter month taken individually (not shown). Since the winter response in AA-2090 remains the same as in November (i.e., equatorward shift of the jet and negative Northern Annular Mode, Figures 2e and S1e), the effect of UTW now reinforces the effect of AA, and a very strong equatorward jet shift/negative NAO is found in TAA-2090 (Figure 2f and S1f). This combined response to UTW and AA differs from the ensemble mean response in CMIP5 and CESM-LENS, which in contrast exhibit reinforced westerlies at the core of the jet (or positive zonal index; see, e.g., Figure 2a in Peings et al., 2018). It is also at odds with results from Butler et al. (2010) and Wang et al. (2012), who found a poleward shift of the eddy-driven jet in response to UTW-type forcing. An explanation for this different response to UTW in winter is found when investigating the polar stratosphere, as described in the next section.

3.2. Role of the Polar Stratosphere in Winter

Figure 3 shows the response of the daily geopotential height over the polar cap (Zcap) in the UTW/AA/TAA-2090 experiments, in a time versus pressure level cross section. Zcap is a proxy for the strength of the polar vortex (Baldwin & Thompson, 2009), with positive (negative) anomalies representing a warmer/weaker (cooler/stronger) polar vortex. Zcap is averaged over the North Atlantic sector here to highlight stratosphere-troposphere coupling in this region, but results are consistent when using the full Zcap. To highlight wave-mean flow interactions in the stratosphere, the superimposed red contours show the associated anomalies in upward planetary wave activity flux entering the stratosphere, derived from the vertical component of the Plumb flux at all levels, averaged between 40°N and 80°N. In order to characterize the associated tropospheric response in the North Atlantic, daily NAO anomalies are shown in the lower panels. In October–November, lower geopotential heights are found in the stratosphere in UTW-2090 (i.e., a cooler and stronger polar vortex), associated with positive NAO values (i.e., reinforced westerly flow) in the North Atlantic (Figure 3a). This signal is opposed to the effect of AA (positive height and negative NAO anomalies,

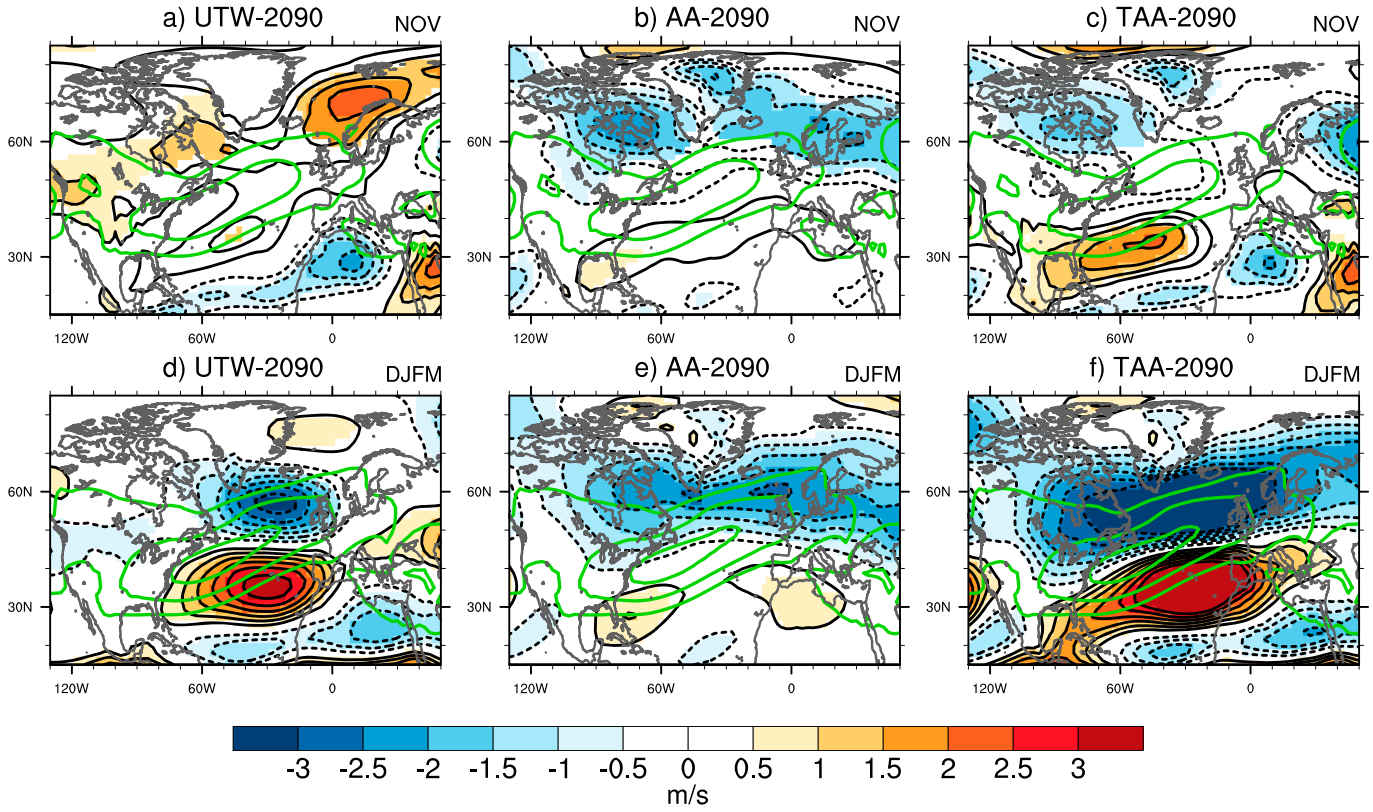

Figure 2. (a) November anomalies of the 700-hPa zonal wind in UTW-2090 (m/s), with climatology shown in green contours (4 m/s interval from 6 m/s). *Shading indicates anomalies that are significant at the 95% confidence level*. (b) Same as (a) but for AA-2090. (c) Same as (a) but for TAA-2090. (d–f) Same as (a–c) but for DJFM anomalies. UTW = upper-troposphere tropical warming; AA = Arctic amplification; DJFM = December to March.

Figure 3b). Note that by design, positive tropospheric height anomalies are found in AA-2090 and TAA-2090 due to the warm anomaly imposed in the Arctic troposphere.

In December, the polar vortex starts to weaken in UTW-2090, following several episodes of upward wave activity flux entering the stratosphere in fall and early winter (Figure 3a, red contours). The anomalous upward wave activity flux originates in the North Atlantic and North Pacific (see the 850-hPa Plumb flux anomalies in Figure S2a). AA-2090 also simulates positive height anomalies in the lower stratosphere (Figure 3b), associated with increased planetary wave activity over Eurasia and the North Pacific (Figure S2b). The large planetary wave forcing in TAA-2090 (Figure S2c) is associated with a strong polar vortex weakening in winter and reinforced negative NAO anomalies from mid-December to end of March (Figure 3c). As revealed by Z50 anomalies in Figure S3, the polar vortex weakens in AA-2090, but in UTW-2090 and TAA-2090 it shifts toward Siberia. In these two experiments, the frequency of sudden stratospheric warming, defined following Charlton and Polvani (2007), more than double in DJFM (13.1 SSW/decade in UTW-2090, 15.3 SSW/decade in TAA-2090, compared to 6.3 SSW/decade in CTL). As expected from stratosphere-troposphere coupling mechanisms (e.g., Kidston et al., 2015), this stratospheric response projects onto the negative NAO near the surface. The response of the stratosphere to UTW is very robust, since similar responses are found when analyzing 10-year subperiods of the UTW-2090 simulation (Figure S4).

The central role of the polar stratosphere is revealed by the -cps experiments with suppressed feedback of the polar stratosphere. The equatorward shift in the eddy-driven jet in UTW-2090-cps is reduced (Figure 4a versus Figure 2d), while it is reinforced in AA-2090-cps (Figure 4b versus Figure 2e). When both forcings are combined, the equatorward shift of the jet is strongly reduced (Figure 4c versus Figure 2f). Figures 4d and 4e illustrate the tug of war between UTW and AA in both set of experiments. They respectively show TAA-2090 minus AA-2090 and TAA-2090-cps minus AA-2090-cps, that is, the isolated effect of UTW in the presence of AA. Unlike in the free polar stratosphere experiments (Figure 4d), in the -cps experiments

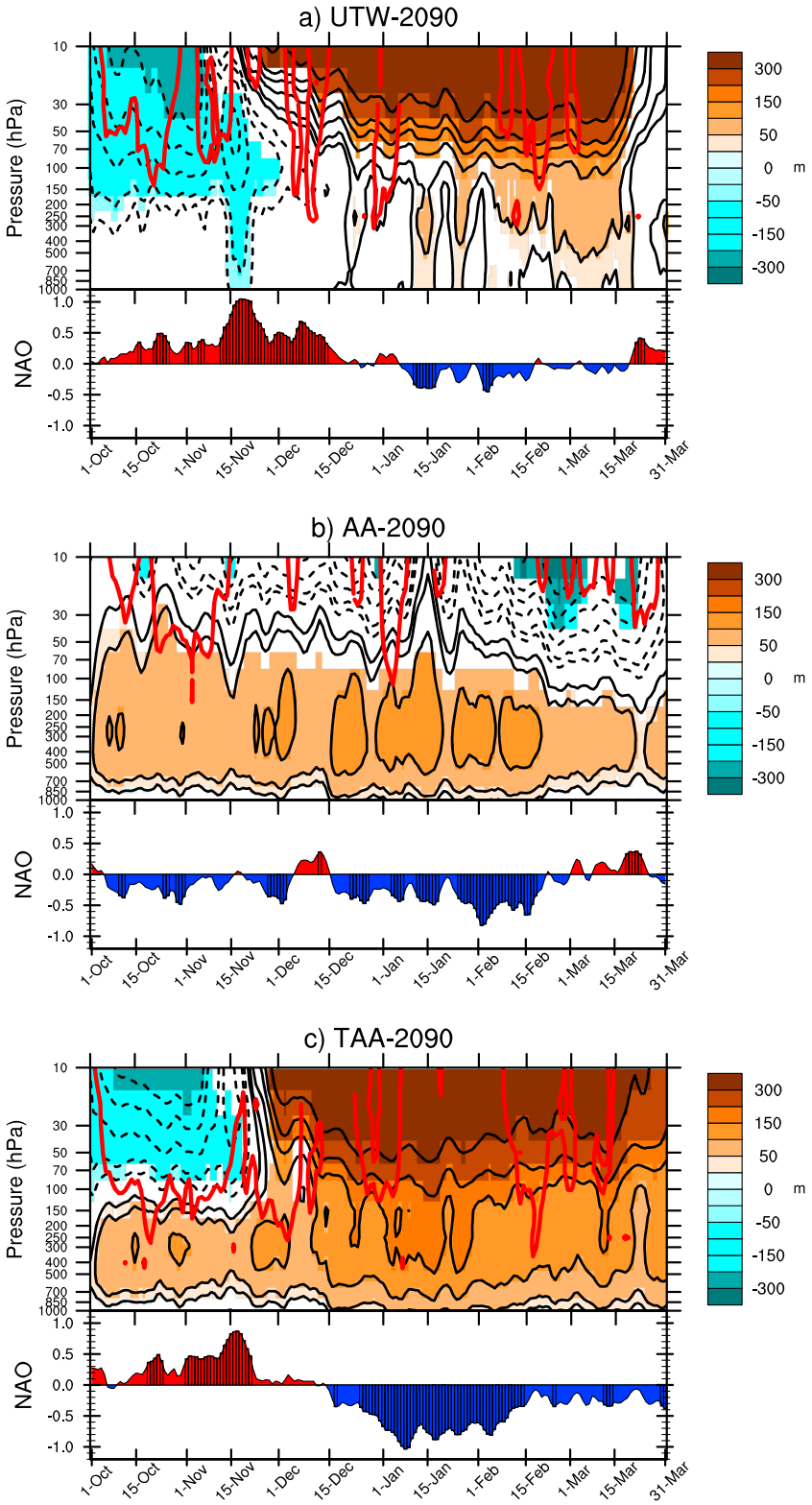

Figure 3. (a) Daily anomalies of North Atlantic Zcap (geopotential height averaged north of 65°N, between 90°W and 30°E), in a time versus pressure level cross section (black contours, 25/50/100/150/200/300 intervals) in UTW-2090. Shading indicates anomalies that are significant at the 95% confidence level. The red contours show upward WAFz pulses in the stratosphere (zonal average between 40°N and 80°N) that are significant at the 95% confidence level (2 standard deviation contour). The bottom panel shows the corresponding daily NAO anomalies, dashed when they are significant at the 95% confidence level. (b) Same as (a) but for AA-2090. (c) Same as (a) but for TAA-2090. UTW = upper-troposphere tropical warming; AA = Arctic amplification; NAO = North Atlantic Oscillation.

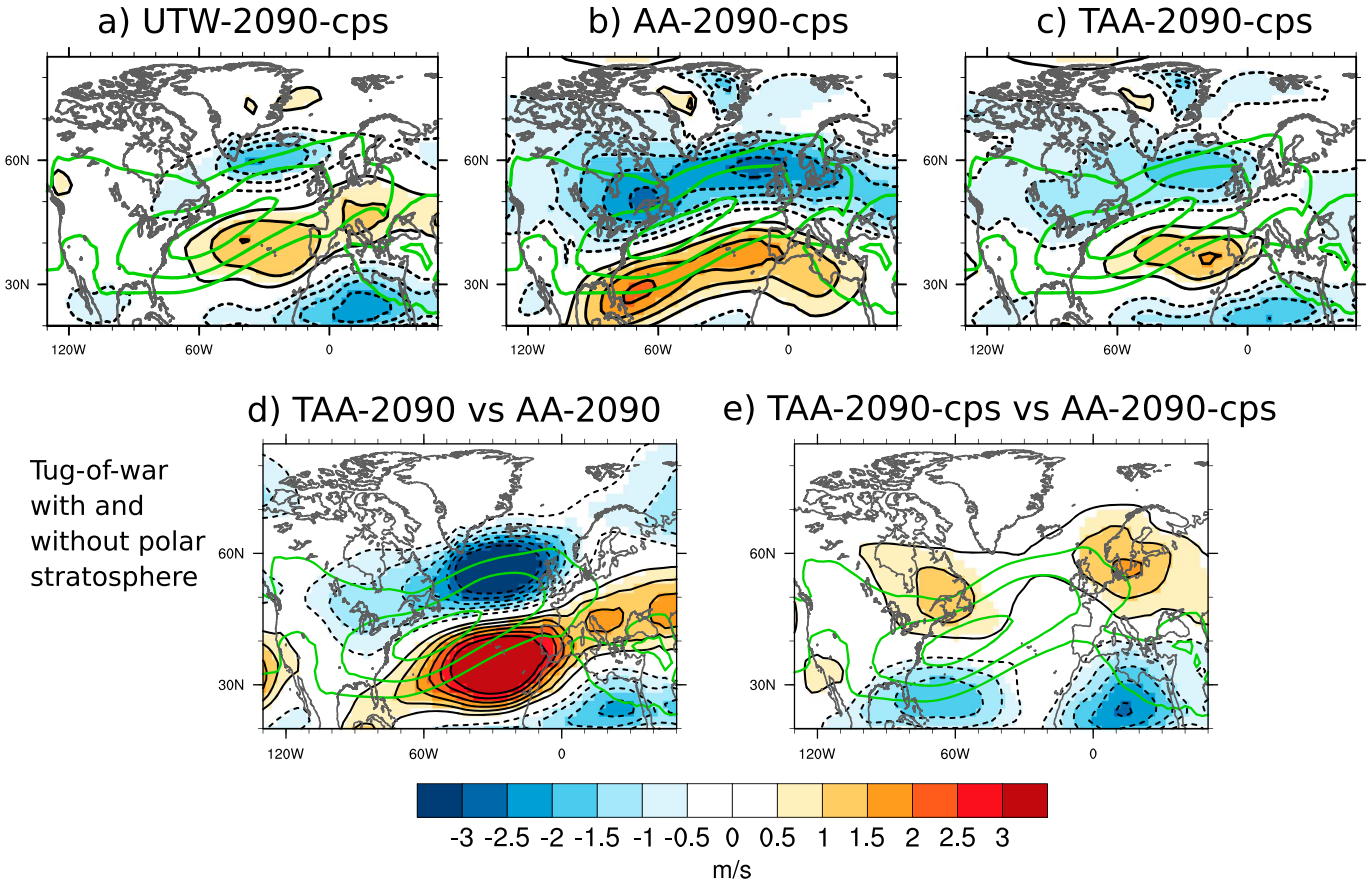

Figure 4. (a) December to March anomalies of the 700-hPa zonal wind in UTW-2090-cps (m/s). (b) Same as (a) but for AA-2090-cps. (c) Same as (a) but for TAA-2090-cps. (d) Tug of war in the *presence* of polar stratospheric feedback (TAA-2090 minus AA-2090). (e) Tug of war in the *absence* of polar stratospheric feedback (TAA-2090-cps minus AA-2090-cps). Climatology is shown in green contours (4 m/s interval from 6 m/s). Shading indicates anomalies that are significant at the 95% confidence level. UTW = upper-troposphere tropical warming; AA = Arctic amplification.

UTW opposes to the effect of AA (Figure 4e versus 4b). Note that there are nonlinearities in the -cps experiments, since the response in TAA-2090 does not equal to the sum of the response to UTW and AA (Figures 4a–4c). As shown in Figure S5, similar change of sign in the tug of war between free and -cps experiments occurs in the North Pacific.

Such influence of the polar stratosphere on North Atlantic climate change projections is consistent with multimodel analyses of RCP8.5 forcing scenarios (e.g.Peings et al., 2017, 2018, Simpson et al., 2018, Zappa & Shepherd, 2017). To illustrate this further, Figure S6 compares the six CMIP5 models/CESM-LENS members with the warmest polar stratosphere anomaly at the end of the 21st century, with the six CMIP5 models/CESM-LENS members with the coolest polar stratosphere anomaly in winter. The U700 anomalies in CMIP5 support the findings of this study, as the "warm polar stratosphere" models exhibit more of an equatorward shift of the eddy-driven jet (Figure S6a), compared to a poleward shift in the "cold polar stratosphere" models (Figure S6b). This is especially visible when the difference between the two ensembles of simulations is computed (Figure S6c), with a dipole of zonal wind anomalies that resembles the winter response in TAA-2090 (Figure 2f), although slightly shifted over Western Europe. In CESM-LENS (Figures S6d–S6f), this modulation by the polar stratosphere is also apparent, even though it is much less detectable due to less variance in this ensemble of simulations that includes only the influence of internal variability (versus internal variability plus model physics in CMIP5).

4. Discussion and Conclusions

This study investigates the tug of war between UTW and AA in terms of their effect on the changes in North Atlantic midlatitude atmospheric circulation at the end of the 21st century. It is the first (to our knowledge)

that attempts to impose UTW and AA anomalies directly into a full AGCM in order to isolate their impact in mid-latitudes. Nudging the temperature in the regions of interest appears to be an efficient way to precisely impose the UTW and AA anomalies and investigate the tropical versus polar tug of war. We opted for temperature forcings representative of the late 21st century (using CESM-LENS to construct the imposed anomalies), but early or mid-21st century forcings may be used in future studies to assess the degree of linearity in the responses. Our main findings can be summarized as follows:

1. AA is associated with increased tropospheric thickness over the Arctic that results in reduced westerlies on the poleward flank of the eddy-driven jet, in line with thermal wind hypotheses (Francis & Vavrus, 2012) and recent Arctic sea ice loss experiments using coupled ocean-atmosphere GCMs (Screen et al., 2018). This tropospheric response is associated with a moderate warming of the polar stratosphere and negative NAO anomalies in winter. A topic of interest in the Arctic-midlatitude linkage field of research is whether AA may increase cold extreme temperature over midlatitudes in winter (Cohen et al., 2014). Figure S7 shows the response in cold extreme temperature, using the cold days index (see definition in the supporting information) that measures both the frequency and intensity of cold extreme days. In our AA-2090 simulation, cold extreme days increase over Siberia and over limited areas of central Europe (Figure S7a). However, no response is found over western Europe and North America. The cooling over Siberia is associated with a high-pressure system that advects polar air into mid-latitudes (see sea level pressure response in Figure S7c), consistent with previous work on the warm Arctic-cold continent pattern (e.g., Mori et al., 2014). The cold anomaly over Siberia is strongly reduced in AA-2090-cps (Figure S7b), as is the high over Siberia (Figure S7d), supporting results from Zhang et al. (2018) and the central role of the polar stratosphere in the warm Arctic-cold Siberia pattern. Note however that in our case the cooling over Siberia is found for a strong pan-Arctic warming, as projected in the future, while the influence of present-day sea ice loss on the warm Arctic-cold Siberia pattern is not evident (Peings, 2019; Sorokina et al., 2016).
2. In autumn, UTW induces a poleward shift of the North Atlantic eddy-driven jet that opposes to the effect of AA, as expected from warmer tropics (e.g., Barnes & Polvani, 2013; Butler et al., 2010; Oudar et al., 2017). However, after the stratospheric polar vortex is well established in winter, a strong polar stratospheric warming emerges that dramatically switches the response of the troposphere in the North Atlantic toward an AA-type response, that is, an equatorward shift of the jet and negative NAO. This constructive influence between the effects of UTW and AA results in larger weakening of the polar vortex and associated negative NAO when both forcings are present. Turning off the influence of the polar stratosphere through nudging further supports this conclusion. In this case the effect of UTW opposes the effect of AA, and we retrieve the tug of war between the effects of UTW and AA identified in previous studies (Butler et al., 2010; Zappa & Shepherd, 2017). Further work is necessary to clarify the stratospheric response to UTW. A source of concern may arise from the fact that present-day SSTs are prescribed underneath the UTW anomaly, which may lead to an unrealistic response due to changing convection and tropospheric stability. However, prescribing future tropical SST to the model without any nudging of the atmosphere yields qualitatively similar results as prescribing UTW (Figure S8), giving us confidence that the UTW-2090 response is not unphysical.

In summary, this study suggests that the polar stratosphere may play a greater role in the future changes of the North Atlantic atmospheric circulation than previously thought. Previous studies using ensembles of RCP8.5 simulations had shown the link between changes in the troposphere (especially in the North Atlantic) and the stratosphere, with some limitations in attributing causality that is inherent to multimodel analyses of coupled ocean-atmosphere simulations (Manzini et al., 2014; Peings et al., 2017, 2018; Zappa & Shepherd, 2017). By isolating the effects of UTW, AA, and of the polar stratosphere feedback, the present sensitivity study complements these multimodel analyses and confirms the active role of the stratosphere in driving the changes in the troposphere. For instance, the strong dependence of the response to UTW on the polar vortex response aligns with the "storyline" analyses of Zappa and Shepherd (2017). Our study also supports the findings of Simpson et al. (2018), who highlighted the role of the polar stratosphere in climate change projections using a similar nudging methodology. By isolating the effects of UTW and AA, we show that the polar stratosphere is particularly sensitive (at least in our model) to UTW and that the stratospheric feedback can strongly affect the response in the North Atlantic westerlies. Whether our results are robust in other GCMs will have to be determined. It will be especially

interesting to explore this question in the new CMIP6 that will include a larger number of models with well-resolved stratosphere than CMIP5.

Acknowledgments
Y. P. and G. M. are supported by the National Science Foundation grant AGS-1624038, the Department of Energy grant DE-SC0019407, and NOAA grant NA15OAR4310164. J. C. is supported by the European H2020 APPLICATE project. Thanks to the NCAR for providing the SC-WACCM model to the community, as well as support for users. Model data used in this study are available on Zenodo (10.5281/zenodo.3066448).

References

Baldwin, M. P., & Thompson, D. W. (2009). A critical comparison of stratosphere–troposphere coupling indices. *Quarterly Journal of the Royal Meteorological Society*, *135*(644), 1661–1672. https://doi.org/10.1002/qj.479

Barnes, E. A., & Polvani, L. M. (2013). Response of the midlatitude jets and of their variability to increased greenhouse gases in the CMIP5 models. *Journal of Climate*, *26*(18), 7117–7135. https://doi.org/10.1175/JCLI-D-12-00536.1

Barnes, E. A., & Polvani, L. M. (2015). CMIP5 projections of Arctic amplification, of the North American/North Atlantic Circulation, and of their relationship. *Journal of Climate*, *28*(13), 5254–5271. https://doi.org/10.1175/JCLI-D-14-00589.1

Blackport, R., & Kushner, P. J. (2017). Isolating the atmospheric circulation response to Arctic Sea ice loss in the coupled climate system. *Journal of Climate*, *30*(6), 2163–2185. https://doi.org/10.1175/JCLI-D-16-0257.1

Butler, A. H., Thompson, D. W., & Heikes, R. (2010). The steady-state atmospheric circulation response to climate change-like thermal forcings in a simple general circulation model. *Journal of Climate*, *23*(13), 3474–3496. https://doi.org/10.1175/2010JCLI3228.1

Cattiaux, J., Peings, Y., Saint-Martin, D., Trou-Kechout, N., & Vavrus, S. (2016). Sinuosity of mid-latitude atmospheric flow in a warming world. *Geophysical Research Letters*, *43*, 8259–8268. https://doi.org/10.1002/2016GL070309

Charlton, A. J., & Polvani, L. M. (2007). A new look at stratospheric sudden warmings. Part I: Climatology and modeling benchmarks. *Journal of Climate*, *20*(3), 449–469. https://doi.org/10.1175/JCLI3996.1

Cohen, J., Screen, J. A., Furtado, J. C., Barlow, M., Whittleston, D., Coumou, D., et al. (2014). Recent Arctic amplification and extreme mid-latitude weather. *Nature Geoscience*, *7*(9), 627–637. https://doi.org/10.1038/ngeo2234

Deser, C., Tomas, R. A., & Sun, L. (2015). The role of ocean–atmosphere coupling in the zonal-mean atmospheric response to Arctic Sea ice loss. *Journal of Climate*, *28*(6), 2168–2186. https://doi.org/10.1175/JCLI-D-14-00325.1

Francis, J. A., & Vavrus, S. J. (2012). Evidence linking Arctic amplification to extreme weather in mid-latitudes. *Geophysical Research Letters*, *39*, L06801. https://doi.org/10.1029/2012GL051000

Harvey, B. J., Shaffrey, L. C., & Woollings, T. J. (2013). Equator-to-pole temperature differences and the extra-tropical storm track responses of the CMIP5 climate models. *Climate Dynamics*, *43*(5-6), 1171–1182. https://doi.org/10.1007/s00382-013-1883-9

Hitchcock, P., & Simpson, I. R. (2014). The downward influence of stratospheric sudden warmings. *Journal of the Atmospheric Sciences*, *71*(10), 3856–3876. https://doi.org/10.1175/JAS-D-14-0012.1

Kay, J. E., Deser, C., Phillips, A., Mai, A., Hannay, C., Strand, G., et al. (2015). The Community Earth System Model (CESM) large ensemble project: A community resource for studying climate change in the presence of internal climate variability. *Bulletin of the American Meteorological Society*, *96*(8), 1333–1349. https://doi.org/10.1175/BAMS-D-13-00255.1

Kidston, J., Scaife, A. A., Hardiman, C., Mitchell, D. M., Butchart, N., Baldwin, M. P., & Gray, L. J. (2015). Stratospheric influence on tropospheric jet streams, storm tracks and surface weather. *Nature Geoscience*, *8*(6), 433–440. https://doi.org/10.1038/ngeo2424

Lu, J., Vecchi, G. A., & Reichler, T. (2007). Expansion of the Hadley cell under global warming. *Geophysical Research Letters*, *34*, L06805. https://doi.org/10.1029/2006GL028443

Manzini, E., Karpechko, A. Y., Anstey, J., Baldwin, M. P., Black, R. X., Cagnazzo, C., et al. (2014). Northern winter climate change: Assessment of uncertainty in CMIP5 projections related to stratosphere-troposphere coupling. *Journal of Geophysical Research: Atmospheres*, *119*, 7979–7998. https://doi.org/10.1002/2013JD021403

McCusker, K. E., Kushner, P. J., Fyfe, J. C., Sigmond, M., Kharin, V. V., & Bitz, C. M. (2017). Remarkable separability of circulation response to Arctic sea ice loss and greenhouse gas forcing. *Geophysical Research Letters*, *44*, 7955–7964. https://doi.org/10.1002/2017GL074327

Mori, M., Watanabe, M., Shiogama, H., Inoue, J., & Kimoto, M. (2014). Robust Arctic sea-ice influence on the frequent Eurasian cold winters in past decades. *Nature Geoscience*, *7*(12), 869–873. https://doi.org/10.1038/ngeo2277

Oudar, T., Sanchez-Gomez, E., Chauvin, F., Cattiaux, J., Terray, L., & Cassou, C. (2017). Respective roles of direct GHG radiative forcing and induced Arctic sea ice loss on the Northern Hemisphere atmospheric circulation. *Climate Dynamics*, *49*(11-12), 3693–3713. https://doi.org/10.1007/s00382-017-3541-0

Peings, Y. (2019). Ural Blocking as a driver of early winter stratospheric warmings. *Geophysical Research Letters*, *46*, 5460–5468. https://doi.org/10.1029/2019GL082097

Peings, Y., Cattiaux, J., Vavrus, S. J., & Magnusdottir, G. (2017). Late twenty-first-century changes in the midlatitude atmospheric circulation in the CESM large ensemble. *Journal of Climate*, *30*(15), 5943–5960. https://doi.org/10.1175/JCLI-D-16-0340.1

Peings, Y., Cattiaux, J., Vavrus, S. J., & Magnusdottir, G. (2018). Projected squeezing of the wintertime North-Atlantic jet. *Environmental Research Letters*, *13*(7), 074016. https://doi.org/10.1088/1748-932/aacc79.

Plumb, R. A. (1985). On the three-dimensional propagation of stationary waves. *Journal of the Atmospheric Sciences*, *42*, 217–229. https://doi.org/10.1175/1520-0469(1985)042<0217:OTTDPO>2.0.CO;2

Rayner, N. A., Parker, D. E., Horton, E. B., Folland, C. K., Alexander, L. V., Rowell, D. P., et al. (2003). Global analyses of sea surface temperature, sea ice, and night marine air temperature since the late nineteenth century. *Journal of Geophysical Research*, *108*(D14), 4407. https://doi.org/10.1029/2002JD002670

Richter, J. H., Sassi, F., & Garcia, R. R. (2010). Toward a physically based gravity wave source parameterization in a general circulation model. *Journal of the Atmospheric Sciences*, *67*(1), 136–156. https://doi.org/10.1175/2009JAS3112.1

Santer, B. S., Solomon, S., Pallotta, G., Mears, C., Po-Chedley, S., Fu, Q., et al. (2017). Comparing tropospheric warming in climate models and satellite data. *Journal of Climate*, *30*(1), 373–392. https://doi.org/10.1175/JCLI-D-16-0333.1

Screen, J. A., Deser, C., Smith, D. M., Zhang, X., Blackport, R., Kushner, P. J., et al. (2018). Consistency and discrepancy in the atmospheric response to Arctic sea-ice loss across climate models. *Nature Geoscience*, *11*(3), 155–163. https://doi.org/10.1038/s41561-018-0059-y

Serreze, M.,. C., Barrett, A. P., Stroeve, J. C., Kindig, D. N., & Holland, M. M. (2009). The emergence of surface-based Arctic amplification. *The Cryosphere*, *3*(1), 11–19. https://doi.org/10.5194/tc-3-11-2009

Shaw, T. A., Baldwin, M., Barnes, E. A., Caballero, R., Garfinkel, C. I., Hwang, Y.-T., et al. (2016). Storm track processes and the opposing influences of climate change. *Nature Geoscience*, *9*(9), 656–664. https://doi.org/10.1038/ngeo2783

Simpson, I. R., Hitchcock, P., Seager, R., Wu, Y., & Callaghan, P. (2018). The downward influence of uncertainty in the Northern Hemisphere stratospheric polar vortex response to climate change. *Journal of Climate*, *31*(16), 6371–6391. https://doi.org/10.1175/JCLI-D-18-0041.1

Smith, K. L., Neely, R. R., Marsh, D. R., & Polvani, L. M. (2014). The Specified Chemistry Whole Atmosphere Community Climate Model (SC-WACCM). *Journal of Advances in Modeling Earth Systems*, *6*, 883–901. https://doi.org/10.1002/2014MS000346

Sorokina, S. A., Li, C., Wettstein, J. J., & Kvamstø, N. G. (2016). Observed atmospheric coupling between Barents Sea Ice and the Warm-Arctic Cold-Siberian Anomaly Pattern. *Journal of Climate*, *29*(2), 495–511. https://doi.org/10.1175/JCLI-D-15-0046.1

Stuecker, M. F., Bitz, C. M., Armour, K. C., Proistosescu, C., Kang, S. M., Xie, S.-P., et al. (2018). Polar amplification dominated by local forcing and feedbacks. *Nature Climate Change*, *8*(12), 1076–1081. https://doi.org/10.1038/s41558-018-0339-y

Taylor, K. E., Stouffer, R. J., & Meehl, G. A. (2012). The CMIP5 experiment design. *Bulletin of the American Meteorological Society*, *93*(4), 485–498. https://doi.org/10.1175/BAMS-D-11-00094.1

Tomas, R. A., Deser, C., & Sun, L. (2016). The role of ocean heat transport in the global climate response to projected Arctic sea ice loss. *Journal of Climate*, *29*(19), 6841–6859. https://doi.org/10.1175/JCLI-D-15-0651.1

Vavrus, S., Wang, F., Martin, J., Francis, J., Peings, Y., & Cattiaux, J. (2017). Changes in North American atmospheric circulation and extreme weather: Evidence of an Arctic connection. *Journal of Climate*, *30*(11), 4317–4333. https://doi.org/10.1175/JCLI-D-16-0762.1

Wang, S., Gerber, E. P., & Polvani, L. M. (2012). Abrupt circulation responses to tropical upper-tropospheric warming in a relatively simple stratosphere-resolving AGCM. *Journal of Climate*, *25*(12), 4097–4115. https://doi.org/10.1175/JCLI-D-11-00166.1

Zappa, G., Pithan, F., & Shepherd, T. G. (2018). Multimodel evidence for an atmospheric circulation response to Arctic sea ice loss in the CMIP5 future projections. *Geophysical Research Letters*, *45*, 1011–1019. https://doi.org/10.1002/2017GL076096

Zappa, G., & Shepherd, T. G. (2017). Storylines of atmospheric circulation change for European regional climate impact assessment. *Journal of Climate*, *30*(16), 6561–6577. https://doi.org/10.1175/JCLI-D-16-0807.1

Zhang, P., Wu, Y., Simpson, I. R., Smith, K. L., Zhang, X., De, B., & Callaghan, P. (2018). A stratospheric pathway linking a colder Siberia to Barents-Kara Sea sea ice loss. *Science Advances*, *4*(7), eaat6025. https://doi.org/10.1126/sciadv.aat6025